Water Research 279 (2025) 123420

Contents lists available at ScienceDirect

Water Research

journal homepage: www.elsevier.com/locate/watres

Nitrous oxide dominates greenhouse gas emissions from hydropower's reservoirs in China from 2020 to 2060

Hongqiao Chen [a], Hengyu Pan [a,*], Shijiang Xiao [b], Shihuai Deng [a]

[a] College of Environmental Sciences, Sichuan Agricultural University-Chengdu Campus, Chengdu, Sichuan 611130, PR China
[b] School of International and Public Affairs, Shanghai Jiao Tong University, Shanghai 200030, China

ARTICLE INFO

Keywords:
Hydropower's reservoirs
Greenhouse gas emissions
Projection
Climate change
Scenario analysis

ABSTRACT

China is ambitious to increase its hydropower share to mitigate climate changes. The greenhouse gas (GHG) emissions from hydroelectric reservoirs may hinder the climate goal. The spatio-temporal patterns of such emissions under future climate changes at the national scale are not clearly addressed. In this study, we evaluate these emissions from 79 hydroelectric reservoirs across China (61.22 % of the national hydropower generation) in 2020, covering carbon dioxide (CO_2), methane (CH_4), and nitrous oxide (N_2O), using the G-res (Greenhouse Gas Reservoir) tool and Integrated Model to Assess the Global Environment–Dynamic Global Nutrient Model (IMAGE-DGNM). A random forest (RF) model is also used to project the emissions in the period of 2020 to 2060 under Shared Socioeconomic Pathway (SSP) scenarios. The results indicate that the carbon intensity (CI) and areal flux varied largely. The reservoirs located in low-altitude areas and older reservoirs generally have higher CIs. N_2O contributed with more than 80 % of the total GHG emission, in which the NH_4^+ concentration is a key factor influencing the N_2O emissions. The projection shows that these emissions will increase by 1.30 %, 6.63 %, and 17.33 % in 2060 compared to 2020 under the SSP119, SSP245, and SSP585 scenarios, respectively, in which CH_4 has the largest growth. Finally, implications toward reduction in such emissions are discussed.

Nomenclature

IHA	International Hydropower Association	YRB	Yangtze River Basin
SLRB	Songhua and Liaohe River Basin	RF	Random forest
CO2	Carbon dioxide	SwB	Southwest Basin
HuRB	Huaihe River Basin	YeRB	Yellow River Basin
N2O	Nitrous oxide	PRB	Pearl River Basin
IPCC	Intergovernmental Panel on Climate Change	CH4	Methane
CI	Carbon intensity	HRB	Haihe River Basin
GRanD	Global reservoir and dam database	SeB	Southeast Basin
SSPs	Shared Socioeconomic Pathways	GHG	Greenhouse gas
IEA	International Energy Agency	CB	Continental Basin
IMAGE-DGNM	Integrated Model to Assess the Global Environment-Dynamic Global Nutrient Model	WRT	Water residence time
GWP	Global Warming Potential	G-res	Greenhouse Gas Reservoir
DLEM	Dynamic Land Ecosystem Model	ResME	Reservoir Methane Emissions
News	Nutrient Export from WaterShed		

(*continued on next column*)

(*continued*)

1. Introduction

To meet the increasing energy demand, hydropower has been identified as one of the climate-friendly sources (Liu et al., 2022). China has a unique advantage to promote its hydropower, owing to the huge theoretical hydropower potential and technically exploitable potential of 694 GW (15 % of the global total) and 542 GW, respectively (Sun et al., 2019). To meet the China's ambitious goal of achieving carbon neutrality in 2060, it has been proposed to enhance the share of hydropower to 20 % of the total energy production in 2050 to reduce the fossil fuel consumption (Liu et al., 2022). However, hydropower's

* Corresponding author.
E-mail address: hengyu@sicau.edu.cn (H. Pan).

https://doi.org/10.1016/j.watres.2025.123420
Received 15 July 2024; Received in revised form 19 February 2025; Accepted 28 February 2025
Available online 1 March 2025

reservoirs, with relatively large storage areas and long operational life compared to other types of reservoirs, result in stable and significant sources of greenhouse gases (GHGs) such as CH_4, CO_2, and N_2O (Fearnside et al., 2012; Harrison et al., 2009; Hendzel et al., 2005; Liu et al., 2011; Rudd et al., 1993), which can hinder the climate mitigation goal. Therefore, evaluation and projection of the spatio-temporal patterns and related drivers of these emissions at the China's national scale can provide further insights toward the climate goal.

Previous estimates indicated annual emissions of 328 Tg CO_2, 22 Tg CH_4, and 0.71 Tg N_2O from global reservoirs (Harrison et al., 2021; Wang et al., 2023), which represent approximately 1.3 % of the anthropogenic CO_2 equivalent emissions globally, which is comparable to those from biomass burning or rice paddies (Li and He, 2022). This highlights the importance for reduction in such emissions. Measurement-based and model-based approaches are commonly employed methods to evaluate these emissions. Floating chamber (Li et al., 2015; Teodoru et al., 2012) and gas chromatograph (Shi et al., 2020) are widely used measurement tools. Previous studies indicated that the emissions evaluated by these measurement-based approaches are significantly lower than the actual emissions as the GHG emissions from bottom water are generally not measured (Adams, 2005; Cheng et al., 2019). Model-based studies can provide more systematic and comprehensive estimations owing to the ability to consider multiple and region-specific factors, such as the hydrological and climatic conditions of the reservoir. Among the various models, such as the generalized linear model (Scherer and Pfister, 2016), Reservoir Methane Emissions (ResME) models (Delwiche et al., 2022), and HydroCalculator Tool (Vilela and Reid, 2017), the Greenhouse Gas Reservoir (G-res) model, based on empirical measurements, is recommend by Intergovernmental Panel on Climate Change (IPCC) for Tier 3 estimates. Levasseur et al. (2021) demonstrated that the G-res model is more appropriate to evaluate CO_2 and CH_4 from hydropower reservoirs. However, reservoirs can emit considerable levels of N_2O (Wang et al., 2023), with a considerably higher global warming potential (GWP), which is not considered in the G-res model. Besides, previous models, including Dynamic Land Ecosystem Model (DLEM) (Li et al., 2024), mechanistic mass balance model (Maavara et al., 2019), and Nutrient Export from WaterShed (News) model (Kroeze et al., 2010), used to calculate N_2O emissions, overlooked emissions from reservoir sediments, while Integrated Model to Assess the Global Environment–Dynamic Global Nutrient Model (IMAGE-DGNM) addresses this gap (Vilmin et al., 2020). In this regard, the integration of both G-res model and IMAGE-DGNM can provide a more holistic information regarding the GHG from reservoirs.

The GHG fluxes from the reservoirs are mainly determined by the related size, age, latitude, operating season, and organic matter of the reservoir (Barros et al., 2011; Beaulieu et al., 2014; Soumis et al., 2004; Tremblay et al., 2004). In this context, the future emissions can be projected considering the significant heterogeneities of these drivers. Soued et al. (2022) used the G-res model to project the cumulative emissions from global reservoirs and reported that the CH_4 bubbling and degassing flux will dominate in the reservoir-induced radiative forcing in the future. Li and He (2022) showed that the GHG emissions of reservoirs can increase approximately 0.11 Pg CO_2 eq yr^{-1} when the dams under construction and planning are considered. However, the climate changes can significantly impact the GHG emissions from reservoirs. For instance, the drawdown of water levels in high-altitude reservoirs, which are located in climate-sensitive area, may increase CH_4 and N_2O emissions (Zhang et al., 2024). Higher temperatures can accelerate the decomposition of organic matter in soils and siltation in reservoirs, increasing the GHG emissions (Yang et al., 2014). An increased precipitation may lead to a higher degree of inundation, promoting anaerobic decomposition of organic matter to produce more GHG emissions (Rosa et al., 2004). The previous studies seldom address the future climate scenario, which may limit the understanding on climate impacts for these emissions. To this end, the Shared Socioeconomic Pathways (SSPs), proposed by IPCC, have been intensively employed to model the future emissions under climate changes.

In summary, the studies on GHG emissions from hydropower reservoirs generally ignored the N_2O emission and impacts of climate change on these emissions. To fill this gap, we estimate the emissions of CH_4, CO_2, and N_2O from 79 hydroelectric reservoirs across China, based on the G-res tool and IMAGE-DGNM. A sensitivity analysis is conducted to ensure reliability of our results. We project the GHG emission of these reservoirs in the period of 2020 to 2060 based on the SSP scenario by using a random forest (RF) model. In addition, we discuss mitigation pathways.

2. Methods

2.1. Study reservoirs

We selected study samples that are regionally representative with available data. The 79 large hydropower stations have an installed capacity exceeding 500 MW, generate 61.22 % of the nation's annual hydropower output, and account for over 52 % of the total national installed hydropower capacity (NEA, 2016). The locations of the studied reservoirs include the China's main basins (Fig. 1): 49 in the Yangtze River Basin (YRB), 4 in the Songhua and Liaohe River Basin (SLRB), 10 in the Southwest Basin (SwB), 7 in the Yellow River Basin (YeRB), 6 in the Pearl River Basin (PRB), and 3 in the Southeast Basin (SeB). Among them, 42 hydropower stations are located at low altitudes (<1000 m), while the others are at high altitudes. The parameters of these hydropower stations, such as the annual energy output, reservoir capacity, and reservoir area, varied largely (Table S1), which can provide more holistic and region-specific results related to their GHG emissions.

2.2. Data sources

The reservoir surface area, reservoir capacity, and geographic locations of existing reservoirs were derived from H. Zhang et al. (2023). Data for the hydropower stations (installed capacity, catchment area, dam height, and power generation) were obtained from National Energy Administration. The average depth, maximum depth, and nitrate content of the reservoir were obtained from previous studies (Guo et al., 2020; Hu et al., 2019; Ji et al., 2022; C. Li et al., 2019; Yue et al., 2017; Zhang et al., 2021; Zhao et al., 2024, 2019; Zhou et al., 2016). The water qualities (water temperature, total phosphorus, dissolved oxygen, ammonia nitrogen, total nitrogen) of the reservoirs were obtained from China National Environmental Monitoring Center. The river length was obtained from China Water Statistical Yearbook (2020). The soil carbon content was obtained from World Soil Information. The cumulative global horizontal radiance was obtained from Geographic Information System Remote Sensing. Monthly meteorological data in the period of 2020 to 2060 and streamflow were obtained from National Tibetan Plateau Data Center. As presented in Table S2, all data used to evaluate the GHG emission in 2020, except the concentration of NO_3^- and dissolved N_2O, are primarily from the year 2020. Owing to the lack of these two data, we sourced them from the literature for study years closest to 2020.

2.3. Methods for calculation of the GHG emissions from reservoirs

2.3.1. Evaluation of the CO_2 and CH_4 emissions from reservoirs

The CO_2 and CH_4 emissions from reservoirs were evaluated by the G-res tool, developed by the International Hydropower Association (IHA) and recommended by IPCC. The G-res tool evaluates the CO_2 diffusive emissions, CH_4 diffusive emissions, CH_4 bubbling emissions, and CH_4 degassing emissions (Prairie et al., 2021). Table 1 shows the factors used to calculate the GHG flux. The equations used in the G-res model have been reported by Prairie et al. (2021).

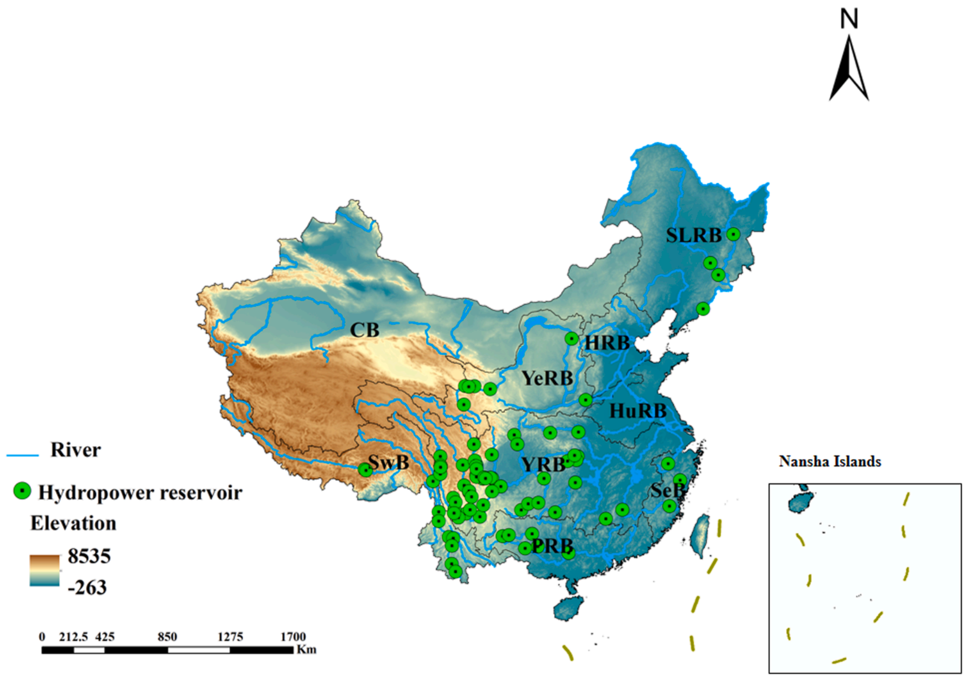

Fig. 1. The location of studied hydropower reservoirs in China.

Table 1
The input factors for calculating the GHG flux.

GHG flux	Factors
CO_2 diffusive emissions	River area before impoundment (%), effective temperature CO_2 (°C), reservoir area (km^2), reservoir soil carbon content (kg C m^{-2}), total phosphorus in the reservoir (μg l^{-1})
CH_4 diffusive emissions	Littoral area (%), effective temperature CH_4 (°C)
CH_4 bubbling emissions	Littoral area (%), reservoir cumulative global horizontal radiance (kg C m^{-2} period^{-1})
CH_4 degassing emissions	Reservoir area (km^2), annual runoff (mm yr^{-1}), catchment area (km^2), CH_4 diffusive emissions (g CO_2 m^{-2} yr^{-1}), water residence time (yr)

2.3.2. Evaluation of N_2O emissions from reservoirs

The N_2O emission calculation for the reservoirs in this study was based on the IMAGE-DGNM model. It has been widely used in simulations of N flows across landscapes and waterscapes (Beusen et al., 2015; Liu et al., 2018). It can simulate biogeochemical cycling of multiple elements and forms in global watersheds by using the speciation of different nutrient sources. IMAGE-DGNM evaluates the nitrification in water (NIT_{N_2O}), denitrification in water ($DENIT_{N_2O}$), incomplete nitrifier denitrification ($NIT\_DENIT_{N_2O}$), nitrification in sediments ($BNIT_{N_2O}$), denitrification in sediments ($BDENIT_{N_2O}$), and N_2O exchange at the water–atmosphere interface ($EXCH_{N_2O}$); detailed calculations consider the supplementary material. For each waterbody type within a grid cell, changes in the amount of inland water N_2O (dN_2O) during the time step (dt) can be expressed in a mass-balanced manner:

$$\frac{dN_2O}{dt} = L_{N_2O} - QC_{N_2O} + NIT_{N_2O} + NIT_{DENITN_2O} + DENIT_{N_2O} + BNIT_{N_2O} + BDENIT_{N_2O} + EXCH_{N_2O}, \tag{1}$$

where L_{N_2O} is the N_2O input to the waterbody (from headwaters, upstream grids, and external groundwater input N_2O and atmospheric deposition input N_2O), Q is the discharge ($m^3 \cdot h^{-1}$), and C_{N_2O} is the inland water dissolved N_2O concentration ($mol \cdot m^{-3}$). The net N_2O production includes nitrification(NIT_{N_2O}), nitrifier denitrification($NIT\_DENIT_{N_2O}$), and denitrification($DENIT_{N_2O}$), which can be positive in the case of net N_2O production, intermediate during an incomplete denitrification, or negative in the case of net N_2O consumption via complete denitrification in the water column and that from nitrification($BNIT_{N_2O}$)and denitrification in the bed sediment ($BDENIT_{N_2O}$). $EXCH_{N_2O}$ is the N_2O exchange at the water−atmosphere interface.

In this study, GHG emissions were converted into carbon footprint based on the GWP. The GWP of N_2O is 298 times the CO_2 equivalent, significantly higher than that of CH_4 (34 times the CO_2 equivalent) in a 100-year time horizon (Liu et al., 2019). The GHG emission intensity of the reservoir is measured by the areal flux rate and carbon intensity (CI) (Almeida et al., 2019; Harrison et al., 2021). The areal flux rate indicates the GHG emission per surface area over a given period (g CO_2 eq m^{-2} yr^{-1}), while the CI is used to evaluate the total GHG emission per generated MWh (kg CO_2 eq MWh^{-1}).

2.4. Projection of GHG emissions from hydropower reservoirs in 2060

The prediction in this study can be classified into the following steps, as shown in Fig. S1. First, both historical data related to air temperature, precipitation, river flow, water quality parameters, reservoir parameters, and sediment parameters from previous studies and predicted data related to air temperature and precipitation based on the SSP scenario were collected. Second, based on the RF model (detailed information considers the supplementary material), 80 % of the dataset related to temperature, precipitation, and river flow was selected as a training set, while the remaining 20 % of the dataset was selected as a test set for model training and validation. Third, the reservoir water temperature and reservoir area were projected according to previous studies (McMahon et al., 2007; Toffolon and Piccolroaz, 2015; H. Zhang et al., 2023). Finally, the G-res model and IMAGE-DGNM were employed to predict the GHG emissions from the reservoir.

GHG emissions from reservoirs may impact China's carbon neutrality target, which necessitates forecasts up to the year 2060. By predicting emissions to 2060, policymakers and stakeholders can prepare more systematic strategies to achieve the carbon neutrality goal. Our climate scenarios essentially cover a range of future climates

(Chapman et al., 2022; Wang et al., 2024; Wu et al., 2024), including SSP119 (lowest vulnerability, lowest mitigation pressure, and lowest anthropogenic radiation forcing), SSP245 (moderate social vulnerability and moderate anthropogenic radiative forcing), and SSP585 (highest artificial radiation forcing), representing contrasting projections of future climate changes.

In this study, we did not consider future changes in power generation mainly owing to the following reasons. The hydropower generation is influenced by fluctuating electricity supply and demand driven by the gross domestic product (GDP) (Qin et al., 2020; Zhou et al., 2020) and electricity prices (Fan et al., 2020); the prediction of these factors can lead to a significant uncertainty, which is beyond the scope of this study. Besides, the accurate projection of hydropower generation under future climate conditions requires detailed monthly historical data on temperature, rainfall, and electricity generation, which are currently unavailable.

3. Results

3.1. GHG emissions from reservoirs in 2020

Fig. 2a presents the CO_2, CH_4, and N_2O areal fluxes from the reservoirs. The studied reservoirs had a wide range of GHG area flux, from 297.18 to 8517.99 g CO_2 eq m^{-2} yr^{-1} (average ± standard deviation = 1900.86 ± 1766.40 g CO_2 eq m^{-2} yr^{-1}) in 2020. N_2O dominated in the GHG emission (81.10 % in terms of CO_2 eq), followed by CO_2 (13.20 %) and CH_4 (5.70 %). The reservoirs of Yantan Plant (8517.99 g CO_2 eq m^{-2} yr^{-1}), Tianshengqiao 1st Plant (7362.62 g CO_2 eq m^{-2} yr^{-1}), and Changheba Plant (7219.38 g CO_2 eq m^{-2} yr^{-1}) were the top three emitters.

Fig. 2b presents the CIs of the reservoirs. The values of the studied reservoirs are 0.006 to 1296.97 kg CO_2 eq MWh^{-1} (average ± standard deviation = 60.19 ± 176.21 kg CO_2 eq MWh^{-1}). The top three hydropower reservoirs with the highest CIs are in Fengman reservoir (1296.97 kg CO_2 eq MWh^{-1}), Danjiangkou reservoir (632.1 kg CO_2 eq MWh^{-1}), and Xinanjiang reservoir (475.1 kg CO_2 eq MWh^{-1}). These reservoirs are older than 50 years. Older reservoirs tend to have higher CIs, primarily due to the decrease in the depth of the reservoir by the accumulation of sediment over time. The reservoir depth is a crucial factor affecting this indicator (Li and He, 2022). Additionally, the increasing age of hydropower stations may negatively impact the power generation efficiency, and further result in an increase in reservoir CI.

At the catchment scale, PRB had the highest GHG areal flux of 4884.24 g CO_2 eq m^{-2} yr^{-1} (Fig. 3a), while YeRB had the lowest, 1588.40 g CO_2 eq m^{-2} yr^{-1}. According to the categories of GHG, YRB had the highest CO_2 areal flux of 524.53 g CO_2 eq m^{-2} yr^{-1}, while YeRB had the lowest, 109.72 g CO_2 eq m^{-2} yr^{-1}. The highest CH_4 areal flux occurred in PRB (300.45 g CO_2 eq m^{-2} yr^{-1}), while the lowest in YeRB (54.97*g* CO_2 eq m^{-2} yr^{-1}). PRB had the highest N_2O areal flux of 4059.25 g CO_2 eq m^{-2} yr^{-1}, while SeB had the lowest, 1086.28 g CO_2 eq m^{-2} yr^{-1}.

Fig. 3b presents that the hydropower reservoir CI varied largely across the China's hydropower reservoirs. Reservoirs in high-altitude regions (>1000 m) generally had lower CIs (average = 18.09 kg CO_2 eq MWh^{-1}), such as those in YRB (13.92) and SwB (15.39), while low-altitude reservoirs had higher CIs (average = 156.39 kg CO_2 eq MWh^{-1}). However, there are several abnormal cases. For example, the value of the Longyangxia hydropower reservoir (altitude = 2582 m) is considerably higher than the average in high-altitude regions, mainly because of its larger area compared to other hydropower stations in high-altitude areas. In general, reservoirs in most high-altitude areas tend to have smaller surface areas. However, the value of the Longyangxia hydropower reservoir is more than 10 times the average in high-altitude regions. The Longyangxia reservoir had a larger surface area primarily as it is the first large-scale cascaded hydropower station on the mainstream of the Yellow River. It has a relatively large installed capacity of 1280 MW. The Shuikou hydropower station is located in a low-altitude area (altitude = 63 m), but its CI (49.5 kg CO_2 MWh^{-1}) is considerably lower than the average in low-altitude reservoirs. The Shuikou Hydropower

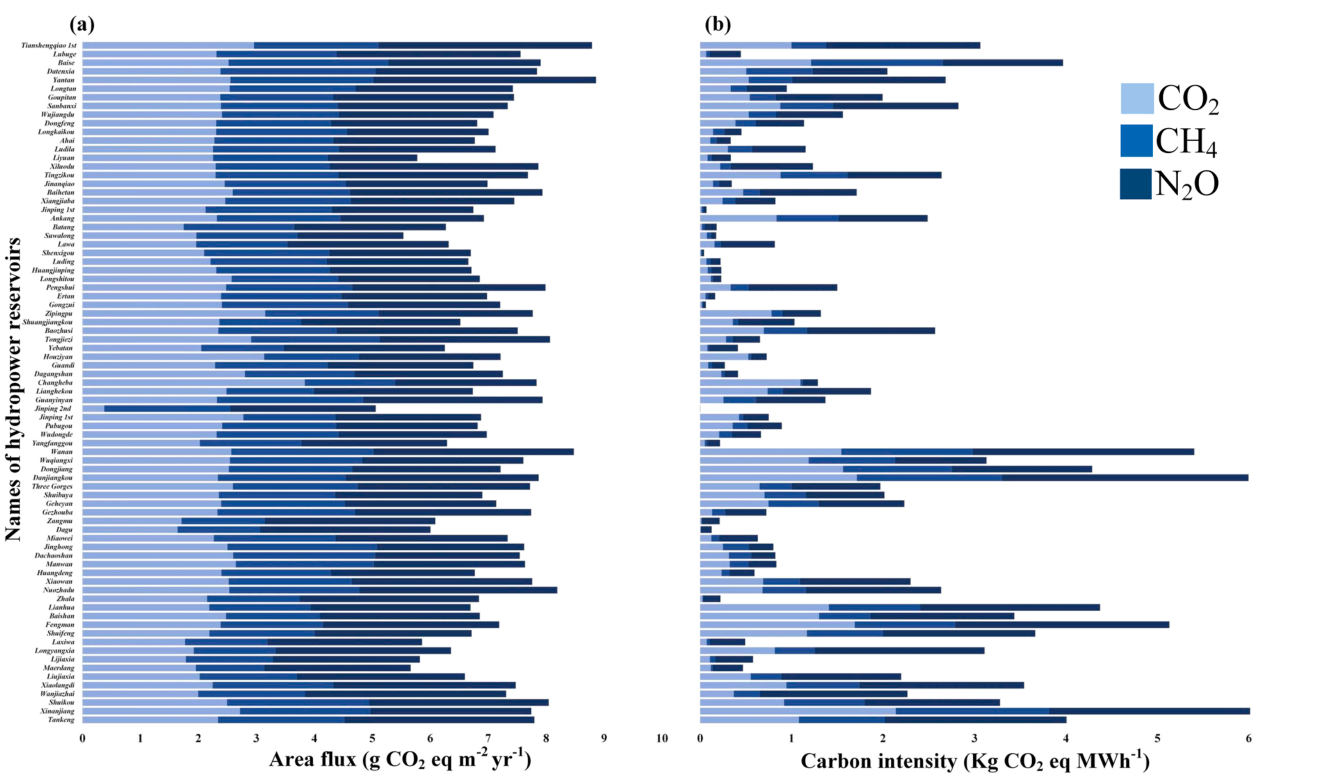

Fig. 2. Emissions intensity of hydropower reservoir. The x-axis represents the results of GHG emissions on a logarithmic scale with a base of 10. (a) areal flux; (b) carbon intensity.

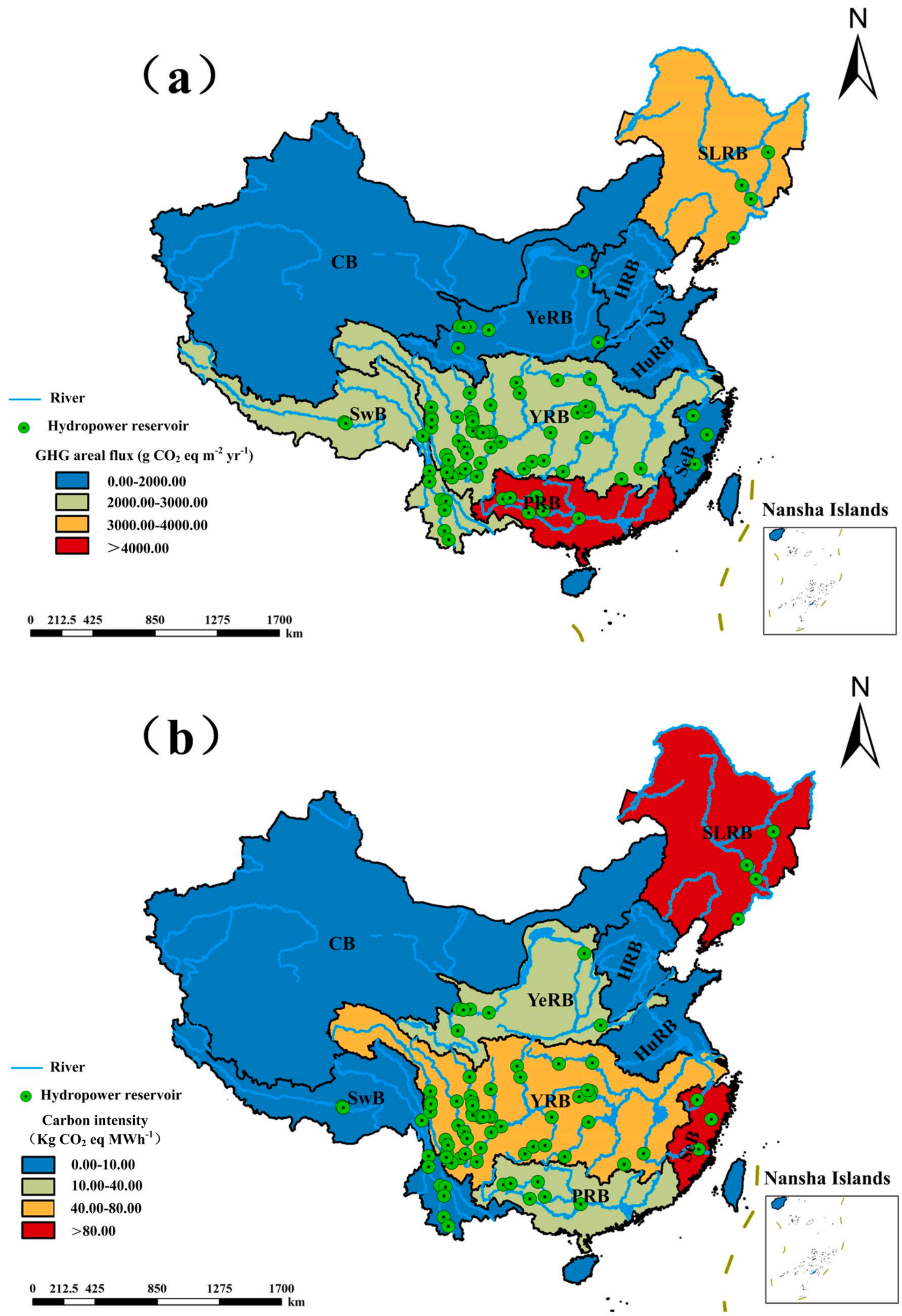

Fig. 3. Emissions intensity from the studied reservoirs at basin scale. (a) GHG areal flux (b) carbon intensity.

reservoir had a lower CI because its installed capacity is 44.10 % larger than the average at the same altitude.

The International Energy Agency (IEA) indicates that a CI from a reservoir lower than 80 kg CO_2 eq MWh^{-1} can be regarded to correspond to a sustainable electricity generation (IHA, 2010). This value is consistent with the energy-related goals of the United Nations 2030 Agenda for Sustainable Development. In this study, 70 reservoirs meet this target, while the average CI of the remaining nine reservoirs is 406.78 kg CO_2 eq MWh^{-1}. This highlights the mitigation potential for those nine reservoirs. In their total emission, N_2O, CO_2, and CH_4 contributed with 86.03 %, 9.55 %, and 4.42 %, respectively. For the other 70 hydroelectric power stations, N_2O, CO_2, and CH_4 contributed with 76.35 %, 16.71 %, and 6.94 % in the total GHG emission, respectively. The proportion of N_2O emissions from those nine hydropower reservoirs is larger. Furthermore, the GWP of N_2O is 298, considerably larger than those of the other two gases. Therefore, the nine hydropower stations that exceed the emission standards need to implement further measures to reduce N_2O emissions.

3.2. Relationship between the reservoirs' GHG emissions and hydropower indicators

As shown in Fig. 4, the installed capacity of hydropower was significantly positively correlated with all GHG pathways except the CH_4

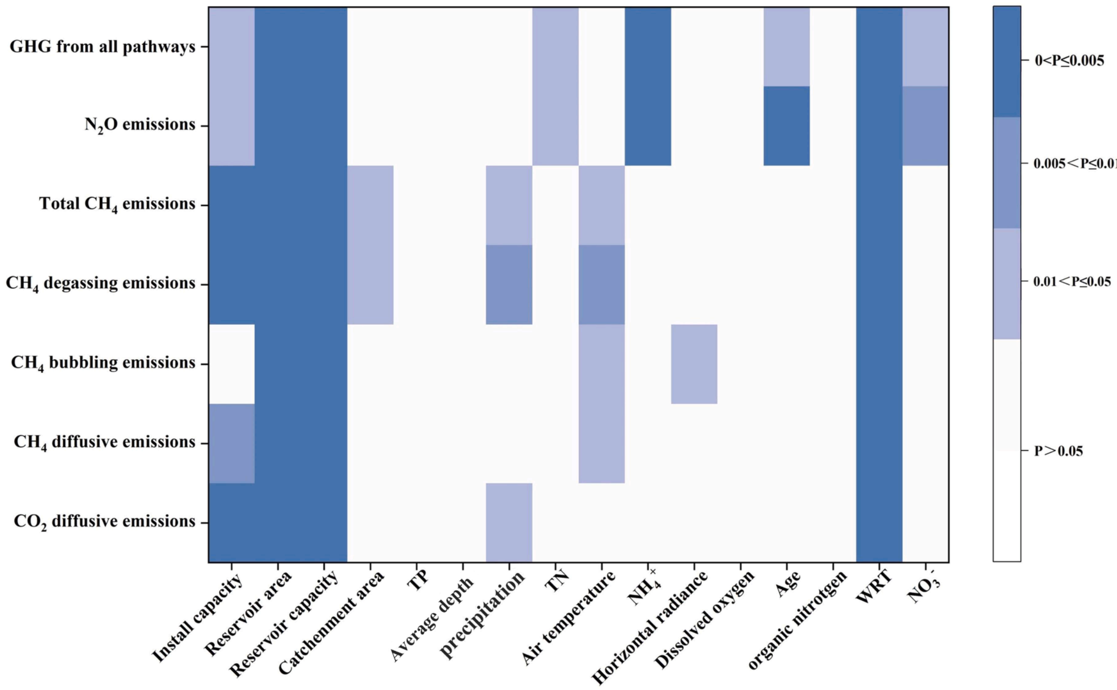

Fig. 4. Heatmap of relationship among GHG emissions and hydropower reservoir indicators. Pearson correlation analysis was employed.

bubbling emissions. This is consistent with the current understanding that the CH_4 bubbling emissions are from CH_4 produced through anaerobic digestion in sediments, which is mainly affected by temperature and hydrostatic pressure (Hertwich, 2013).The CO_2 diffusive emissions exhibit highly significant positive correlations with the reservoir area, reservoir capacity, and Water residence time (WRT) ($P \leq 0.005$) and weak positive correlation with the precipitation ($P \leq 0.05$). The CH_4 diffusive emissions exhibit highly significant positive correlations with the reservoir area, reservoir capacity, and WRT. The CH_4 bubbling emissions have highly significant positive correlations with the reservoir area, reservoir capacity, and WRT and weak positive correlations with the air temperature and horizontal radiation. The CH_4 degassing emissions exhibit highly significant positive correlations with the reservoir area, reservoir capacity, and WRT, significant positive correlations with the precipitation and air temperature ($P \leq 0.01$), and weak positive correlation with the hydropower station-controlled catchment area. The total CH_4 emissions exhibit highly significant positive correlations with the reservoir area, reservoir capacity, and WRT and weak positive correlations with the precipitation, air temperature, and hydropower station-controlled catchment area. The N_2O emissions have highly significant positive correlations with the reservoir area, reservoir capacity, reservoir NH_4^+ concentration, age, and WRT, significant positive correlation with the reservoir NO_3^- concentration, and weak positive correlation with the total nitrogen concentration. The total GHG emissions exhibit highly significant positive correlations with the reservoir area, reservoir capacity, reservoir NH_4^+ concentration, and WRT, which suggests that these four indicators have a key role in the GHG emissions from the studied reservoirs.

3.3. Projected GHG emissions from reservoirs

As shown in Fig. 5, 1959 sample data related to temperature, precipitation, and river flow (accounting for 80 % of the dataset) were selected as a training set, while the remaining 490 samples (accounting for 20 % of the dataset) were selected as a test set for model training and validation. The results indicated a high degree of accuracy with $R^2 =$

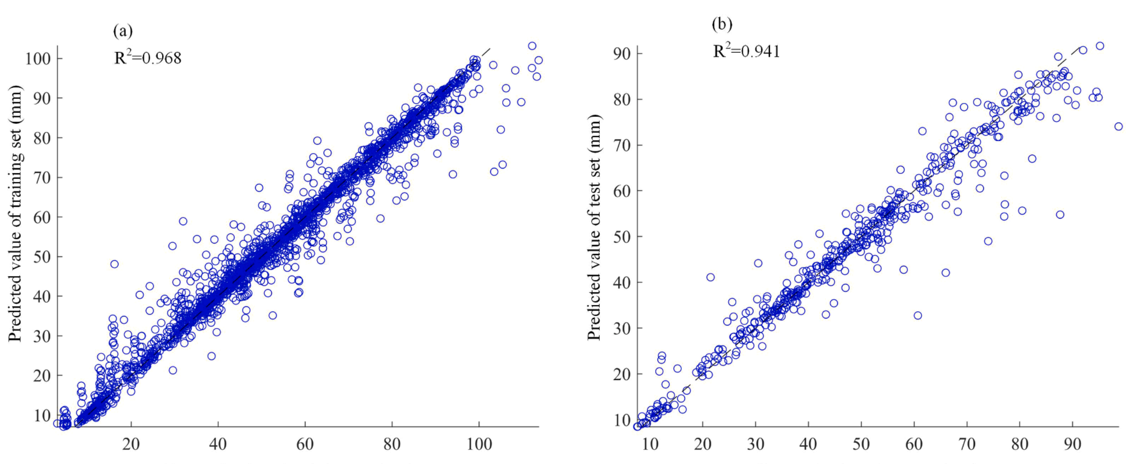

Fig. 5. Simulations of streamflow for hydropower reservoirs by RF model. (a) and (b) present the results of training and validation processes, respectively.

0.97 for the training set. Similarly, the test set had a satisfactory performance, with $R^2 = 0.94$. Thus, the prediction under future climate changes through RF is reliable.

In 2020, the GHG emissions from the studied reservoirs were 17.66 Tg CO_2 eq yr^{-1}. As shown in Fig. 6a, under the SSP119 scenario in 2025, the GHG emissions decrease to 17.07 Tg CO_2 eq yr^{-1}, increase to 17.85 Tg CO_2 eq yr^{-1} in 2030, decrease to 17.07 Tg CO_2 eq yr^{-1} in 2035, rebound to 18.21 Tg CO_2 eq yr^{-1} in 2040, and slowly decrease to 18.04 Tg CO_2 eq yr^{-1} in 2045. By 2050, the emissions reach a peak of 18.71 Tg CO_2 eq yr^{-1}, followed by a gradual decrease over the next decade to 17.89 Tg CO_2 eq yr^{-1}. In contrast, as shown in Fig. 6b, under SSP245 in 2025, the GHG emissions decrease to 17.09 Tg CO_2 eq yr^{-1}, increase to 17.25 Tg CO_2 eq yr^{-1} in 2030, decrease again to 17.16 Tg CO_2 eq yr^{-1} in 2035, rebound to 18.00 Tg CO_2 eq yr^{-1} in 2040, and decrease to 17.18 Tg CO_2 eq yr^{-1} in 2045. Over the following 15 years, the emissions gradually increase, reaching a peak of 18.83 Tg CO_2 eq yr^{-1} in 2060. As shown in Fig. 6c, under SSP585, the GHG emissions decrease to 17.37 Tg CO_2 eq yr^{-1} in 2025, and then gradually increase. In 2060, the emissions reach a peak of 21.02 Tg CO_2 eq yr^{-1}.

The variation in GHG emissions across basins is notable under the studied scenarios. Under the SSP119 scenario, the emissions of the SeB, YRB, and PRB reservoirs fluctuate for the first 30 years, and ultimately decrease but still exceed the current emission levels (Fig. 6a). On the other hand, the emissions from the reservoirs in SLRB, YeRB, and SwB decrease in the period of 2020 to 2035, followed by an increase in the period of 2035 to 2040, and stabilize by 2060. Notably, by 2060, the reservoirs in SLRB and YeRB are predicted to have lower GHG emissions than their current levels. Conversely, the reservoirs in YRB and PRB are expected to emit slightly more GHG emissions than the current level, while the reservoirs in SwB will maintain their current emission levels. In Fig. 6b, under the SSP245 scenario, the SeB, SLRB, YeRB, SwB, YRB, and PRB reservoirs exhibit fluctuations for the first 40-year period. By 2060, only SLRB is expected to have lower GHG emissions than the current levels. Finally, under the SSP585 scenario (Fig. 6c), the emissions from the reservoirs in YRB and PRB experience slight decreases in the period of 2020 to 2025, followed by sharp increases. The reservoirs in SeB, SLRB, YeRB, and SwB fluctuate over the next 20 years, and gradually surpass the 2020 emission levels.

According to GHG category, Fig. 6d shows that, by 2060, CH_4 and CO_2 increase by 19.97 % and 17.14 %, respectively, under the SSP119 scenario. However, the N_2O emission fluctuates and decreases to 13.95 Tg CO_2 eq yr^{-1} in 2060. Fig. 6e shows that, compared to 2020, the N_2O and CH_4 emissions in 2060 are expected to increase by 4.76 % and 51.08 % under the SSP245 scenario, respectively, while the CO_2 emissions are predicted to decrease by 1.17 %. Fig. 6f illustrates a significant increase in GHG emissions, among which the N_2O, CH_4, and CO_2 emissions are predicted to increase by 11.02 %, 81.10 %, and 41.34 % in 2060 under the SSP585 scenario, respectively.

4. Discussion

4.1. *Environmental factors and their effects on GHG emissions from reservoirs*

Our results show that N_2O contributed with more than 80 % of the total GHG emissions in 2020. The above correlation analysis shows that the NH_4^+ concentration in the reservoir mainly from agriculture and industry is an important factor affecting the N_2O emissions from hydropower reservoirs. The first step of nitrification is to oxidize NH_4^+ to NH_2OH and generate N_2O and NO_2^- simultaneously. NH_2OH is then further oxidized to N_2O or NO_2^- is reduced to N_2O. In other words, NH_4^+ promotes N_2O production in the reservoir when a sufficient content of NH_4^+ is available (Cheng et al., 2019; Liu et al., 2017). This indicates potential N_2O mitigation strategies by reducing the NH_4^+ concentration. Besides, high nitrogen loads due to agricultural runoff can also significantly increase the N_2O emissions (Huang et al., 2024).

Notably, we did not observe significant variations in CO_2 emissions and CH_4 emissions with the reservoir age, compared to other studies (Barros et al., 2011). However, we revealed a significant correlation between the reservoir age and N_2O emissions, which has been seldom reported previously. As the reservoir ages, the river carries more sediment into the reservoir. The nitrification and denitrification of sediments are strengthened and result in an increase in N_2O emissions.

Further, the water residence time is an important factor affecting the

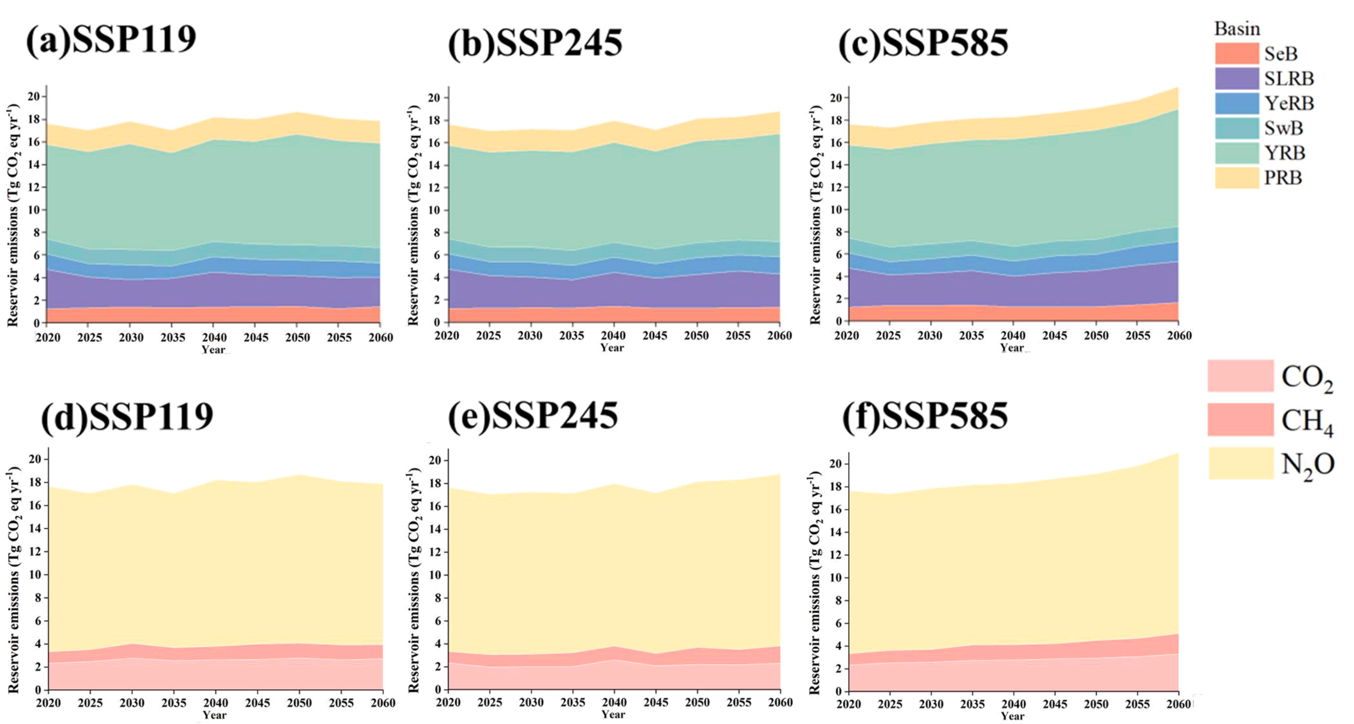

Fig. 6. Projected GHG emissions from reservoir categorized by basin (a, b, c) and GHG category (d, e, f).

GHG from all pathways, which is consistent with the report by IHA (2010). When the water residence time is longer, the organic matter in the water body has more time to decompose. These organic matters, under the action of microorganisms, are converted into CO_2, CH_4, and other products through various biochemical reactions. Therefore, a longer water residence time promotes the emission of CO_2 and CH_4. N_2O is also one of the products of further transformation of NO_2^-, an intermediate product in the nitrification process. The extension of hydraulic retention time may provide more time for nitrifying bacteria to oxidize NH_4^+ into NO_2^-, and thereby increase the potential for N_2O generation. N_2O can also be produced during the denitrification process, particularly when denitrification conditions are incomplete (presence of dissolved oxygen, insufficient C/N ratio, etc.).

The pivotal role of air temperature in influencing GHG emissions in reservoirs has been reported (DelSontro et al., 2010; Kankaala et al., 2004; Xing et al., 2005; Yang et al., 2014). An increase in air temperature can expedite the decomposition of organic carbon, and thereby foster higher GHG emissions. Furthermore, the optimal water temperature for CH_4 production is approximately 25 °C (Dunfield et al., 1993), while, for denitrification and nitrification reactions in water, the optimal water temperatures are 25 and 23 °C, respectively (Garnier, J., 2000). For benthic nitrification and denitrification reactions, the optimal water temperature is 20 °C (Billen et al., 2015). Therefore, in the range where bacteria can tolerate fluctuations, the production of CH_4 and N_2O increases with the water temperature. Owing to the highest water temperature tolerance of methane-producing bacteria, this can also explain the highest increase in methane in future climate changes.

The GHG emissions from reservoirs align with the overarching trend of climate change. The comparison of the present weather state to future scenarios reveals a significant increase in the annual average air temperature. Under the SSP585 scenario, the annual average air temperature has the largest increase (3.55 °C), and, accordingly, the GHG emissions from the reservoir increase most significantly (an increase of 3.36 Tg CO_2 eq yr^{-1}). In addition, among various future climate scenarios, the GHG emission growth rate of the SwB reservoir is lowest (0.34 %, 1.20 %, and 1.34 %), likely as the air temperature increase in SwB is slowest.

4.2. Comparison to previous studies

There are numerous studies on evaluations of GHGs from hydropower reservoirs, which generally ignored the N_2O emissions (Li and He, 2022; Li et al., 2015). Our study fills this gap by considering N_2O. Table 2 compares previous estimates to our results, which can be divided into model-based and measurement-based results. The results varied due to different methods and data sets of estimation. Lauerwald et al. (2019) estimated that the N_2O emission flux from the global reservoirs is 62.94 g CO_2 eq m^{-2} yr^{-1} based on the method of Maavara et al. (2019). This estimate is considerably lower than our estimate of 1665.8 g CO_2 eq m^{-2} yr^{-1}, as they did not consider the nitrification and denitrification of sediment, which contributed with almost half of the total N_2O emissions in this study. Most notable are the reservoirs of Baishan, Guanyinyan, and Lubuge, which account for more than 65 % of the total N_2O emissions. The process of generation of N_2O in reservoir sediments mainly involves microbial nitrification and denitrification, whereby N_2O is produced under aerobic conditions by nitrifying bacteria in the process of converting NH_4^+ to NO_3^- (He et al., 2017). Numerous studies have also shown that nitrification and denitrification in sediments are important sources of N_2O emissions (Deutsch et al., 2010; Usui et al., 2001). The N_2O emissions evaluated by Li et al. (2018) and Deemer et al. (2016) by measurement-based approaches are considerably lower than ours, which can be explained as many commonly used techniques for measurement of aquatic GHG emissions focus on quantification of the diffusion flux of gases at the air–water interface. For N_2O, the primary flux pathway is based on the high solubility in water (with a molar fraction solubility of 5.07×10^{-4} at 20 °C). Consequently, the N_2O emissions obtained through these measurement-based approaches are significantly lower than the actual N_2O emissions from reservoirs, as measurement-based approaches cannot include the whole emissions of reservoirs by setting sampling points. For instance, when hydroelectric power plants are dredged, the churning of large amounts of sediment in reservoirs also increases the N_2O emissions, which may be ignored by the measurement-based approaches (Cheng et al., 2019).

Our simulation results for CO_2 emission from reservoirs are close to those of Deemer et al. (2016) and Hertwich (2013) (Table 2). This supports the applicability of our G-res model-based approach. Li et al. (2015) employed a hybrid method by combining measurement-based and model-based approaches to predict CO_2 and CH_4 emissions from a hydropower reservoir. They estimated that the CO_2 emissions are roughly twice higher than those in our study, as they did not consider the emission before the reservoir construction, which was considered with the G-res tool. Li et al. (2018) estimated that the CO_2 emissions from China reservoirs are also twice higher than ours, as most of their reservoirs were in low-altitude areas. Most of the reservoirs in this study were located in high-altitude areas, with 2–3 freezing months annually. Freezing effects can significantly decrease GHG emissions from reservoirs (Boereboom et al., 2012). Under the freezing effect, the ice on the surface of the reservoir blocks the gas exchange at the water–gas interface, which includes the exchange of oxygen with the reservoir water as well as the emission of CO_2. In addition, the freezing effect reduces the microbial activity, which, in turn, reduces the CO_2 emission.

The CH_4 emissions estimated by Li et al. (2015) are half of ours, mainly because they did not consider CH_4 degassing emissions. Our study demonstrates that CH_4 degassing emissions contributed with 52.50 % of the total CH_4 emissions. The CH_4 diffusion emissions and CH_4 bubbling emissions estimated in this study (62.95 g CO_2 eq m^{-2} yr^{-1}) are close to those of Li et al. (2015). A detailed description on CH4 degassing has been reported by Hertwich (2013).

Table 2
Comparison of results with earlier studies Estimates of GHG emissions from hydropower reservoirs.

	Area	Areal flux			Method	Source
	(10^6 km^2)	CO_2	CH_4	N_2O		
		g CO_2 eq m^{-2} yr^{-1}				
China's 79 reservoirs	0.02	362.99	132.54	1665.8	Model	This study
China reservoirs	0.03	712.65	169.60	173.66	Measurement	Li et al., 2018
Global reservoirs	0.25			62.94	Model	Lauerwald et al., 2019
Global reservoirs	0.31	441.65	1985.6	51.28	Measurement	Deemer et al., 2016
China reservoirs	0.03	867.24	65.52		Measurement and model	Li et al., 2015
Boreal reservoirs	0.08	970	1360		Model	Hertwich, 2013
Temperate reservoirs	0.13	420	288		Model	Hertwich, 2013
Tropical reservoirs	0.12	1200	1840		Model	Hertwich, 2013
Temperate reservoirs	0.9	511	248.2		Measurement	St. Louis et al., 2000
Tropical reservoirs	0.6	1277.5	3723		Measurement	St. Louis et al., 2000

4.3. Uncertainty analysis

Common sensitivity analysis methods include local sensitivity analysis and global sensitivity analysis (Borgonovo and Plischke, 2016). Global sensitivity analysis is the recommended method in the field of hydrology (Pappenberger et al., 2008), because, compared to local methods, global methods offer specific advantages, including the ability to simultaneously consider the impact of changes in each parameter on the model output across the entire parameter range, and high degree of adaptability to nonlinear and nonmonotonic models. Therefore, we employ a global sensitivity analysis to verify the uncertainty of the results, with the widely used Sobol' method (Ganji et al., 2016).

Parameters involved in GHG emission calculations, obtained from measurements or modeling (Fig. 7), can increase the degree of uncertainty. Therefore, the sensitivity of these parameters was tested based on a Sobol sensitivity analysis with 4000 sample points.

As shown in Fig. 7a, the effect index of the reservoir soil carbon content (0.74) on the CO_2 emissions was largest, followed by those of the reservoir area (0.29), river area before impoundment (0.25), air temperature (0.19), and total phosphorus (0.01). The air temperature has the largest effect index for CH_4 emissions (Fig. 7b), accounting for 48.43 % of the total effect index, followed by the littoral area (18.12 %), WRT (13.99 %), and catchment area (11.69 %), while the other factors together account for only 7.77 %. The water temperature, reservoir area, and NH_4^+ were the top three factors for N_2O emissions (Fig. 7c), which contributed with 89.43 % of the total effect index.

Based on the sensitivity analysis results, the confidence interval was explored by a Monte Carlo simulation under a change of ±30 %. The results of 10,000 samples are normally distributed; the highest bar represents the highest frequency (Fig. 8). To quantify the uncertainty, we utilized a confidence interval of 5 % to 95 %.

As shown in Fig. 8a, the 95 % confidence interval of CO_2 annual emissions ranged from 2.02×10^7 to 4.05×10^7 kg CO_2 yr^{-1}. The highest-frequency value (2.92×10^7 kg CO_2 yr^{-1}) is close to our calculated result (mean value: 2.95×10^7 kg CO_2 yr^{-1}). In Fig. 8b, the 95 % confidence interval of CH_4 annual emissions ranges from 9.67×10^6 to 1.61×10^7 kg CO_2 eq yr^{-1}. The highest-frequency value of 1.24×10^7 kg CO_2 eq yr^{-1} is also close to our calculated result (1.27×10^7 kg CO_2 eq yr^{-1}). Fig. 8c shows that the 95 % confidence interval of N_2O annual emissions ranges from 1.03×10^8 to 2.51×10^8 kg CO_2 eq yr^{-1}. The highest-frequency value (1.75×10^8 kg CO_2 eq yr^{-1}) is close to our calculated result of 1.81×10^8 kg CO_2 eq yr^{-1}. In summary, the Sobol sensitivity analysis and Monte Carlo simulations demonstrate the reliability of our results.

4.4. Mitigation of GHG emissions from hydropower reservoirs

Although previous studies generally indicated that the GHG emission intensity of hydropower is considerably lower than that of thermal power generation (Feng et al., 2014; Hondo, 2005), our results demonstrate that the considerable GHG emissions from hydropower reservoirs, ignored in previous studies, should be carefully considered, as they can hinder the climate mitigation goal, particularly as China will continue to develop the hydropower according to the 14th Five-Year Plan. By 2030, the installed capacity of hydropower is expected to reach approximately 370 million kW. Below, we suggest strategies to reduce the GHG emissions from reservoirs.

For existing hydropower reservoirs, targeted measures should be employed considering their specific emission pathways and characteristics. Our results show that the N_2O dominates in the GHG emissions, particularly for the nine reservoirs that cannot meet the IEA's target for a sustainable hydropower. In addition, regular maintenance of equipment and dredging of reservoirs are necessary. Notably, China has already begun to consider the issue of sediment deposition in older hydropower reservoirs. In 2021, sediment deposition was enacted for a large hydropower station on the Yellow River (Zhou et al., 2021). However, the sediment is still the main factor driving GHG emissions in the studied reservoirs, which requires more specific solutions. For instance, the N_2O emissions from sediments in the Baishan, Xinanjiang, and Lubuge reservoirs account for more than 65 % of the N_2O emissions. Measures such as scouring of the lower riverbed to expel and reduce the sediment should be implemented for these reservoirs.

Finally, considering the significant positive correlation between NH_4^+ and NO_3^- with N_2O emissions from reservoirs, measures need to be implemented to improve the water quality and mitigate the eutrophication (for example, by reducing artificial nutrient inputs and applying sludge removal treatments). Reservoirs with high NO_3^- and NH_4^+ concentrations, such as those in Xiaolangdi Reservoir, Fengman Reservoir,

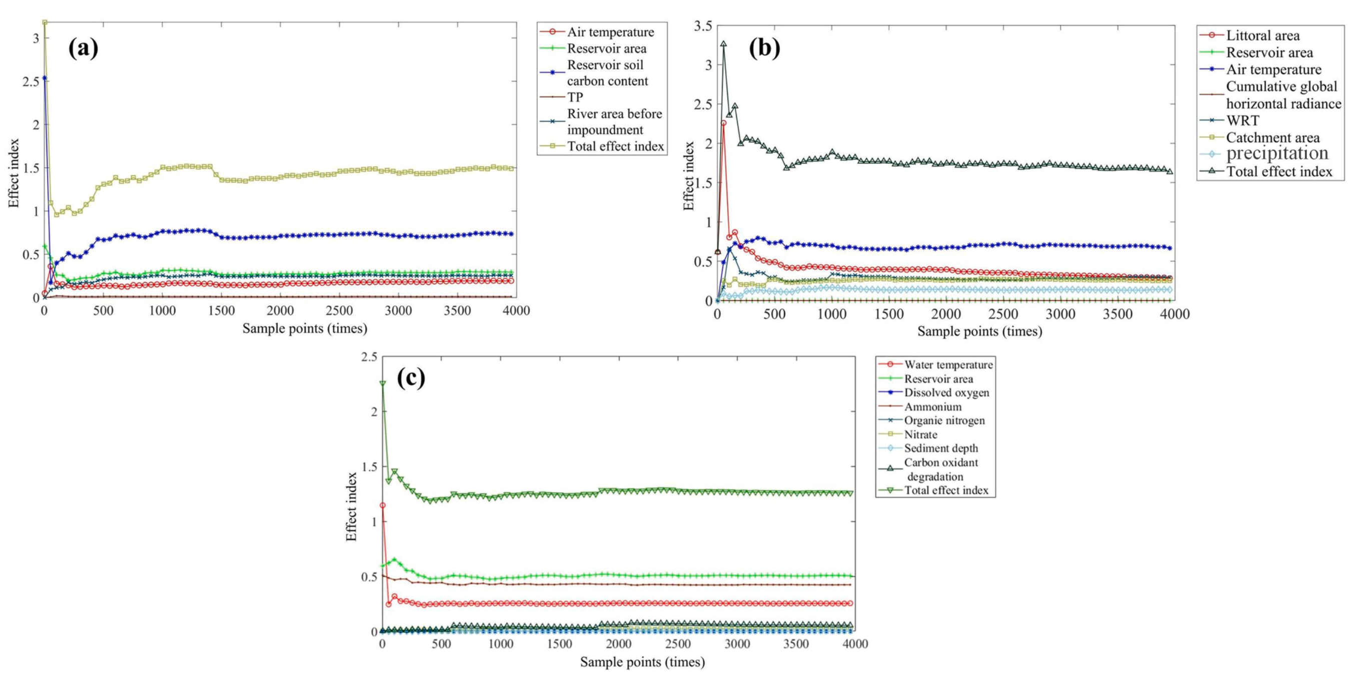

Fig. 7. The Sobol' total effect indexes of GHG emission. (a) CO_2;(b) CH_4;(c) N_2O.

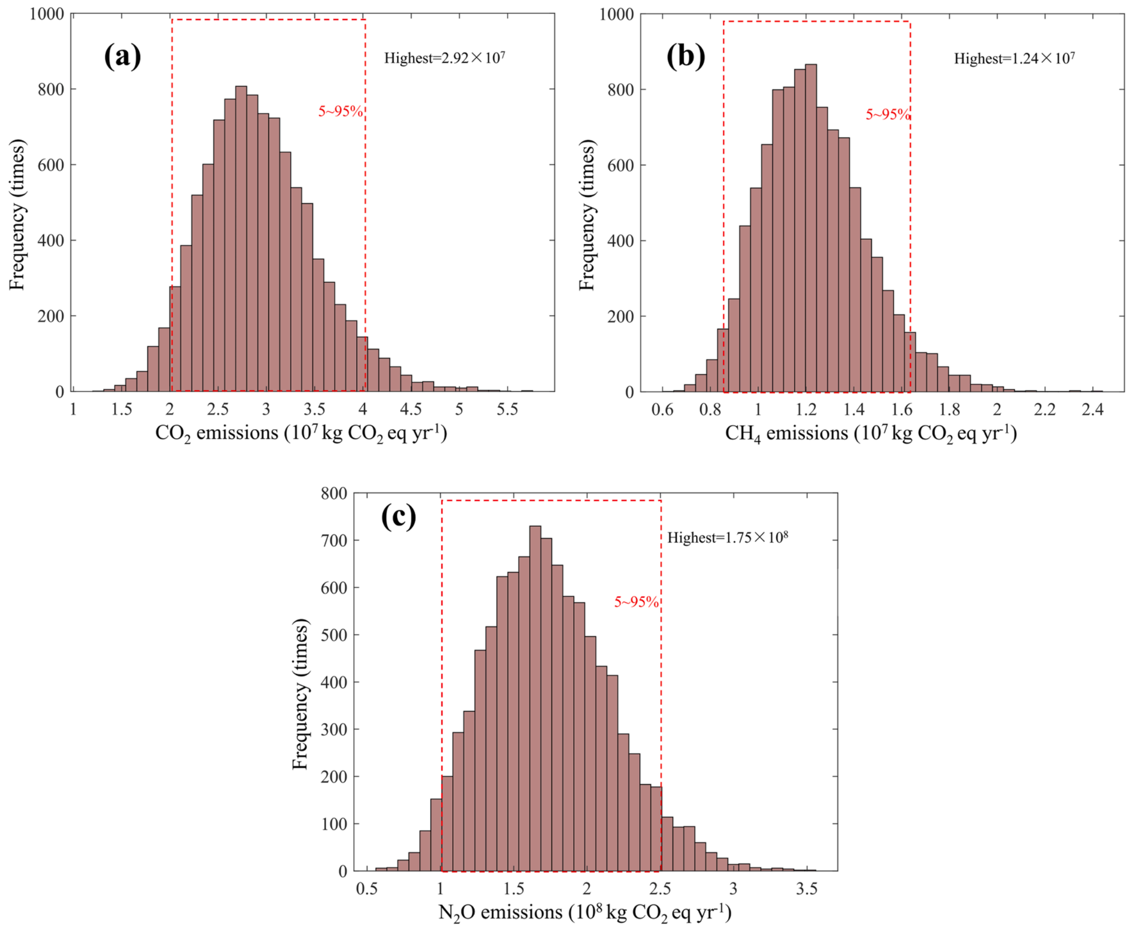

Fig. 8. The uncertainty analysis results of GHG emissions. (a) CO_2;(b) CH_4;(c) N_2O.

and Tingzikou Reservoir (Fig. S2), are generally located in China's major grain-producing areas. However, these areas are still exposed to an excessive application of nitrogen fertilizers, which can result in higher concentrations of NO_3^- and NH_4^+. Although China implemented measures, including organic and chemical fertilizers, straw recycling, and deep placement of fertilizers, to reduce the agricultural non-point-source pollution (Duan et al., 2024), the pollution in flood areas such as reservoirs should be carefully considered.

For the future hydropower development, our study demonstrates that reservoirs in high-altitude areas generally have lower CIs, and that the steeper terrain in high-elevation areas can favor hydropower projects with higher power densities (Almeida et al., 2019). This provides insightful implications for the future hydropower planning with respect to GHG emission reduction. This also requires to consider other important issues such as biodiversity, ecosystem service, and geological factors. In the design and operation of reservoirs, it is essential to fully consider the potential impact of hydraulic retention time on GHG emissions and employ corresponding measures to reduce these emissions. For instance, optimization of reservoir dispatching, increase in water body mobility, and improvement in water quality can effectively mitigate the adverse effects of long hydraulic retention times on GHG emissions.

4.5. Limitations and prospect of this study

As for previous studies conducted at national and global scales, our estimates of GHG emissions from China's hydropower reservoirs are inevitably impacted by data limitations and uncertainties. In this study, we did not encompass all hydropower reservoirs in China primarily due to data deficiencies, which potentially hinders a comprehensive understanding of GHG emissions from hydropower reservoirs. However, more than 60 % of the country's hydropower generation across all basins was included in this study. Our study also ignores the impact of future changes in air temperature and precipitation on the water quality, which may lead to uncertainty of our projection to some degree. The prediction of changes in TP, NH_4^+, organic nitrogen, dissolved oxygen, and other factors, mainly resulting from the social and economic development, under the climate changes requires involvement of multiple complex models, in which large uncertainties can emerge. The accurate prediction of socioeconomic development is beyond the scope of this study. Additionally, our projections did not cover all SSP scenarios, though the most representative scenarios were considered. Finally, our data on NO_3^- and N_2O in reservoirs were sourced from the literature rather than from measurements, which may increase the uncertainty associated with our findings. However, the uncertainty analysis demonstrated the reliability of our results.

As subjects of future researches, the establishment or enhancement of reservoir-related monitoring systems can include more hydropower reservoirs and collect more specific data, which can provide a more holistic understanding of the impact of climate changes on GHG emissions from reservoirs and related flooded land. In addition, the development of interdisciplinary models integrating climate, energy supply and demand, geoscience, and socioeconomic system can provide more accurate and region-specific results. Finally, a broader range of climate scenarios should be considered in the future to elucidate more detailed emission pathways and provide related mitigation strategies.

5. Conclusion

Mitigation of GHG emissions from hydropower reservoirs has been widely recognized, especially given that China's ambitious goal to increase its hydropower share. Uncovering and projecting the spatial-temporal pattern of these emissions can therefore prepare insightful implications towards sustainable hydropower. However, previous studies seldomly consider future climate impacts on these emissions. This study fills this gap by combining G-res tool, IMAGE-DGNM and random forest model based on SSP scenarios. 79 hydropower, contributing more than 60 % of the nation's total hydropower generation and across main China's basins, were taken as study cases. We observed significant spatial heterogeneity of GHG emission intensity, in which reservoirs with lower CI were generally located in high altitude area. N_2O dominates these GHG emissions, followed by CO_2 and CH_4. The projection further suggests that these emissions will increase under all the three scenarios, in which CH_4 has the greatest increase due largely to it is more sensitive to air temperature. Finally, this study provides insightful suggestions to reduce these emissions that have global implications.

CRediT authorship contribution statement

Hongqiao Chen: Writing – original draft, Methodology, Investigation. **Hengyu Pan:** Writing – review & editing, Writing – original draft, Supervision, Methodology, Funding acquisition, Data curation, Conceptualization. **Shijiang Xiao:** Writing – review & editing, Validation, Methodology. **Shihuai Deng:** Supervision.

Declaration of competing interest

The authors declare that they have no known competing financial interests or personal relationships that could have appeared to influence the work reported in this paper.

Acknowledgements

This study is supported by the National Natural Science Foundation of China (Grant No. 72204179).

Supplementary materials

Supplementary material associated with this article can be found, in the online version, at doi:10.1016/j.watres.2025.123420.

Data availability

Data will be made available on request.

References

Adams, D.D., 2005. Diffuse flux of greenhouse gases — methane and carbon dioxide — at the sediment-water interface of some lakes and reservoirs of the world. Greenh. Gas Emiss. Fluxes Process. 1, 129–153.
Almeida, R.M., Shi, Q., Gomes-Selman, J.M., Wu, X., Xue, Y., Angarita, H., Barros, N., Forsberg, B.R., García-Villacorta, R., Hamilton, S.K., Melack, J.M., Montoya, M., Perez, G., Sethi, S.A., Gomes, C.P., Flecker, A.S., 2019. Reducing greenhouse gas emissions of Amazon hydropower with strategic dam planning. Nat. Commun. 10.
Barros, N., Cole, J.J., Tranvik, L.J., Prairie, Y.T., Bastviken, D., Huszar, V.L.M., Del Giorgio, P., Roland, F., 2011. Carbon emission from hydroelectric reservoirs linked to reservoir age and latitude. Nat. Geosci. 4, 593–596.
Beaulieu, J.J., Smolenski, R.L., Nietch, C.T., Townsend-Small, A., Elovitz, M.S., 2014. High methane emissions from a midlatitude reservoir draining an agricultural watershed. Environ. Sci. Technol. 48, 11100–11108.
Beusen, A.H.W., Van Beek, L.P.H., Bouwman, A.F., Mogollón, J.M., Middelburg, J.J., 2015. Coupling global models for hydrology and nutrient loading to simulate nitrogen and phosphorus retention in surface water - Description of IMAGE-GNM and analysis of performance. Geosci. Model. Dev. 8, 4045–4067.
Billen, G., Garnier, J., Silvestre, M., 2015. A simplified algorithm for calculating benthic nutrient fluxes in river systems. Ann. Limnol. 51, 37–47.
Boereboom, T., Depoorter, M., Coppens, S., 2012. Gas properties of winter lake ice in Northern Sweden: implication for carbon gas release. Biogeosciences 9, 827–838.
Borgonovo, E., Plischke, E., 2016. Sensitivity analysis: a review of recent advances. Eur. J. Oper. Res. 248, 869–887.
Chapman, S., Birch, C.E., Marsham, J.H., Part, C., Hajat, S., Chersich, M.F., Ebi, K.L., Luchters, S., Nakstad, B., Kovats, S., 2022. Past and projected climate change impacts on heat-related child mortality in Africa. Environ. Res. Lett. 17.
Cheng, F., Zhang, H.M., Zhang, G.L., Liu, S.M., Song, G.D., Du, G.X., 2019. Distribution and emission of N 2 O in the largest river-reservoir system along the Yellow River. Sci. Total Environ. 666, 1209–1219.
Deemer, B.R., Harrison, J.A., Li, S., Beaulieu, J.J., Delsontro, T., Barros, N., Bezerra-Neto, J.F., Powers, S.M., Dos Santos, M.A., Vonk, J.A., 2016. Greenhouse gas emissions from reservoir water surfaces: a new global synthesis. Bioscience.
DelSontro, T., McGinnis, D.F., Sobek, S., Ostrovsky, I., Wehrli, B., 2010. Extreme methane emissions from Swiss hydropower reservoir. Environ. Sci. Technol. 44, 2419–2425.
Delwiche, K.B., Harrison, J.A., Maasakkers, J.D., Sulprizio, M.P., Worden, J., Jacob, D.J., Sunderland, E.M., 2022. Estimating driver and pathways for hydroelectric reservoir methane emissions using a new mechanistic model. J. Geophys. Res. Biogeosciences 127, 1–24.
Deutsch, B., Forster, S., Wilhelm, M., Dippner, J.W., Voss, M., 2010. Denitrification in sediments as a major nitrogen sink in the Baltic Sea: an extrapolation using sediment characteristics. Biogeosciences 7, 3259–3271.
Duan, J., Liu, H., Zhang, X., Ren, C., Wang, C., Cheng, L., Xu, J., Gu, B., 2024. Agricultural management practices in China enhance nitrogen sustainability and benefit human health. Nat. Food 5, 378–389.
Dunfield, P., knowles, R., Dumont, R., Moore, T.R., 1993. Methane production and consumption in temperate and subarctic peat soils: response to temperature and pH. Soil Biol. Biochem. 25, 321–326.
Fan, J.L., Hu, J.W., Zhang, X., Kong, L.S., Li, F., Mi, Z., 2020. Impacts of climate change on hydropower generation in China. Math. Comput. Simul. 167, 4–18.
Fearnside, P.M., Pueyo, S., 2012. Greenhouse-gas emissions from tropical dams. Nat. Clim. Chang. 2, 382–384.
Feng, K., Hubacek, K., Siu, Y.L., Li, X., 2014. The energy and water nexus in Chinese electricity production: a hybrid life cycle analysis. Renew. Sustain. Energy Rev. 39, 342–355.
Ganji, A., Maier, H.R., Dandy, G.C., 2016. A modified Sobol' sensitivity analysis method for decision-making in environmental problems. Environ. Model. Softw. 75, 15–27.
Garnier, J., Billen, G., Palfner, L., 2000. Understanding the oxygen budget and related ecological processes in the river Mosel: the RIVERSTRAHLER approach. Hydrobiologia 410, 151–166.
Guo, X., Tang, Y., Xu, Y., Zhang, S., Ma, J., Xiao, S., Ji, D., Yang, Z., Liu, D., 2020. Using stable nitrogen and oxygen isotopes to identify nitrate sources in the Lancang River, upper Mekong. J. Environ. Manage. 274, 111197.
Harrison, J.A., Maranger, R.J., Alexander, R.B., Giblin, A.E., Jacinthe, P.A., Mayorga, E., Al, E., 2009. The regional and global significance of nitrogen removal in lakes and reservoirs. Biogeochemistry 93, 143–157.
Harrison, J.A., Prairie, Y.T., Mercier-Blais, S., Soued, C., 2021. Year-2020 Global Distribution and pathways of reservoir methane and carbon dioxide emissions according to the greenhouse gas from reservoirs (G-res) Model. Glob. Biogeochem. Cycles 35.
He, Q., Zhu, Y., Li, G., Fan, L., Ai, H., Huangfu, X., Li, H., 2017. Impact of dissolved oxygen on the production of nitrous oxide in biological aerated filters. Front. Environ. Sci. Eng. 11.
Hendzel, L., Matthews, C., Venkiteswaran, J., St Louis, V., Burton, D., Joyce, E., Bodaly, R., 2005. Nitrous oxide fluxes in three experimental boreal forest reservoirs. Environ. Sci. Technol. 39, 4353–4360.
Hertwich, E.G., 2013. Addressing biogenic greenhouse gas emissions from hydropower in LCA. Environ. Sci. Technol. 47, 9604–9611.
Hondo, H., 2005. Life cycle GHG emission analysis of power generation systems: Japanese case. Energy 30, 2042–2056.
Hu, M., Wang, Y., Du, P., Shui, Y., Cai, A., Lv, C., Bao, Y., Li, Y., Li, S., Zhang, P., 2019. Tracing the sources of nitrate in the rivers and lakes of the southern areas of the Tibetan Plateau using dual nitrate isotopes. Sci. Total Environ. 658, 132–140.
Huang, S., Zhang, P., Zheng, W., Zhang, J., Li, Y., Wang, Y., Jiang, E., Liu, S., Xia, X., 2024. Characteristics and influencing factors of greenhouse gas emissions from reservoirs in the Yellow River Basin: a Meta-analysis. Sci. China Earth. Sci. 67 (7).
IHA, 2010. GHG Measurement Guidelines For Freshwater Reservoirs. (International Hydropower Association).
Ji, X., Shu, L., Li, J., Zhao, C., Chen, W., Chen, Z., Shang, X., Dahlgren, R.A., Yang, Y., Zhang, M., 2022. Tracing nitrate sources and transformations using △17O, δ15N, and δ18O-NO3− in a coastal plain river network of eastern. China. J. Hydrol. 610, 127829.
Kankaala, P., Ojala, A., Käki, T., 2004. Temporal and spatial variation in methane emissions from a flooded transgression shore of a boreal lake. Biogeochemistry 68, 297–311.
Kroeze, C., Dumont, E., Seitzinger, S., 2010. Future trends in emissions of N2O from rivers and estuaries. J. Integr. Environ. Sci. 7, 71–78.
Lauerwald, R., Regnier, P., Figueiredo, V., Enrich-Prast, A., Bastviken, D., Lehner, B., Maavara, T., Raymond, P., 2019. Natural lakes are a minor global source of N2O to the atmosphere. Glob. Biogeochem. Cycles 33, 1564–1581.
Levasseur, A., Mercier-Blais, S., Prairie, Y.T., Tremblay, A., Turpin, C., 2021. Improving the accuracy of electricity carbon footprint: estimation of hydroelectric reservoir greenhouse gas emissions. Renew. Sustain. Energy Rev. 136.
Li, C., Li, S.L., Yue, F.J., Liu, J., Zhong, J., Yan, Z.F., Zhang, R.C., Wang, Z.J., Xu, S., 2019. Identification of sources and transformations of nitrate in the Xijiang River using nitrate isotopes and Bayesian model. Sci. Total Environ. 646, 801–810.
Li, M., He, N., 2022. Carbon intensity of global existing and future hydropower reservoirs. Renew. Sustain. Energy Rev. 162.

Li, S., Bush, R.T., Santos, I.R., Zhang, Q., Song, K., Mao, R., Wen, Z., Lu, X.X., 2018. Large greenhouse gases emissions from China's lakes and reservoirs. Water. Res. 147, 13–24.
Li, S., Zhang, Q., Bush, R.T., Sullivan, L.A., 2015. Methane and CO_2 emissions from China's hydroelectric reservoirs: a new quantitative synthesis. Environ. Sci. Pollut. Res. 22, 5325–5339.
Li, Y., Tian, H., Yao, Y., Shi, H., Bian, Z., Shi, Y., Wang, S., Maavara, T., Lauerwald, R., Pan, S., 2024. Increased nitrous oxide emissions from global lakes and reservoirs since the pre-industrial era. Nat. Commun. 15, 1–11.
Liu, Y., Zhu, R., Ma, D., Xu, H., Luo, Y., Huang, T., Sun, L., 2011. Temporal and spatial variations of nitrous oxide fluxes from the littoral zones of three alga-rich lakes in coastal Antarctica. Atmos. Environ. 45, 1464–1475.
Liu, X., Beusen, A.H.W., Van Beek, L.P.H., Mogollón, J.M., Ran, X., Bouwman, A.F., 2018. Exploring spatiotemporal changes of the Yangtze River (Changjiang) nitrogen and phosphorus sources, retention and export to the East China Sea and Yellow Sea. Water. Res. 142, 246–255.
Liu, X., Li, S., Wang, Z., Han, G., Li, J., Wang, B., Wang, F., Bai, L., 2017. Nitrous oxide (N2O) emissions from a mesotrophic reservoir on the Wujiang River, southwest China. Acta Geochim 36, 667–679.
Liu, X., Xiao, S., Pan, H., Zheng, X., Han, W., Huang, C., Deng, S., 2022. Optimizing hydropower plants based on carbon-water-energy-ecosystem nexus. Energy Convers. Manag. 270.
Liu, X., Zhou, T., Liu, Y., Zhang, X., Li, L., Pan, G., 2019. Effect of mid-season drainage on CH4 and N2O emission and grain yield in rice ecosystem: a meta-analysis. Agric. Water Manag. 213, 1028–1035.
Maavara, T., Lauerwald, R., Laruelle, G.G., Akbarzadeh, Z., Bouskill, N.J., Van Cappellen, P., Regnier, P., 2019. Nitrous oxide emissions from inland waters: are IPCC estimates too high? Glob. Chang. Biol. 25, 473–488.
McMahon, T.A., Pegram, G.G.S., Vogel, R.M., Peel, M.C., 2007. Revisiting reservoir storage-yield relationships using a global streamflow database. Adv. Water Resour. 30, 1858–1872.
NEA, 2016. 13rd Five-year" Plan for Hydropower Development. National Energy Administration of China.
Pappenberger, F., Beven, K.J., Ratto, M., Matgen, P., 2008. Multi-method global sensitivity analysis of flood inundation models. Adv. Water Resour. 31, 1–14.
Prairie, Y.T., Mercier-Blais, S., Harrison, J.A., Soued, C., Giorgio, P.del, Harby, A., Alm, J., Chanudet, V., Nahas, R., 2021. A new modelling framework to assess biogenic GHG emissions from reservoirs: the G-res tool. Environ. Model. Softw. 143, 105117.
Qin, P., Xu, H., Liu, M., Xiao, C., Forrest, K.E., Samuelsen, S., Tarroja, B., 2020. Assessing concurrent effects of climate change on hydropower supply, electricity demand, and greenhouse gas emissions in the Upper Yangtze River Basin of China. Appl. Energy 279, 115694.
Rosa, L.P., Dos Santos, M.A., Matvienko, B., Dos Santos, E.O., Sikar, E., 2004. Greenhouse gas emissions from hydroelectric reservoirs in tropical regions. Clim. Change 66, 9–21.
Rudd, J.W.M., Hecky, R.E., Harris, R., Kelly, C.A., 1993. Are hydroelectric reservoirs significant sources of greenhouse gases. Ambio 22, 246–248.
Scherer, L., Pfister, S., 2016. Hydropower's biogenic carbon footprint. PLoS One 11.
Shi, W., Chen, Q., Zhang, J., Liu, D., Yi, Q., Chen, Y., Ma, H., Hu, L., 2020. Nitrous oxide emissions from cascade hydropower reservoirs in the upper Mekong River. Water. Res. 173, 115582.
Soued, C., Harrison, J.A., Mercier-Blais, S., Prairie, Y.T., 2022. Reservoir CO2 and CH4 emissions and their climate impact over the period 1900–2060. Nat. Geosci. 15, 0–7.
Soumis, N., Duchemin, É., Canuel, R., Lucotte, M., 2004. Greenhouse gas emissions from reservoirs of the western United States. Glob. Biogeochem. Cycles 18.
St. Louis, V.L., Kelly, C.A., Duchemin, É., Rudd, J.W.M., Rosenberg, D.M., 2000. Reservoir surfaces as sources of greenhouse gases to the atmosphere: a global estimate. Bioscience 50, 766–775.
Sun, X., Wang, X., Liu, L., Fu, R., 2019. Development and present situation of hydropower in China. Water Policy. 21, 565–581.
Teodoru, C.R., Bastien, J., Bonneville, M.C., Del Giorgio, P.A., Demarty, M., Garneau, M., Hélie, J.F., Pelletier, L., Prairie, Y.T., Roulet, N.T., Strachan, I.B., Tremblay, A., 2012. The net carbon footprint of a newly created boreal hydroelectric reservoir. Glob. Biogeochem. Cycles 26.
Toffolon, M., Piccolroaz, S., 2015. A hybrid model for river water temperature as a function of air temperature and discharge. Environ. Res. Lett. 10.
Tremblay, A., Lambert, M., Gagnon, L., 2004. Do hydroelectric reservoirs emit greenhouse gases? Environ. Manage. 33.
Usui, T., Koike, I., Ogura, N., 2001. N2O production, nitrification and denitrification in an estuarine sediment. Estuar. Coast. Shelf Sci. 52, 769–781.
Vilela, T., Reid, J., 2017. Improving hydropower choices via an online and open access tool. PLoS. One 12, e0179393.
Vilmin, L., Mogollón, J.M., Beusen, A.H.W., van Hoek, W.J., Liu, X., Middelburg, J.J., Bouwman, A.F., 2020. Modeling process-based biogeochemical dynamics in surface fresh waters of large watersheds with the IMAGE-DGNM Framework. J. Adv. Model. Earth Syst. 12, 1–19.
Wang, J., Vilmin, L., Mogollón, J.M., Beusen, A.H.W., van Hoek, W.J., Liu, X., Pika, P.A., Middelburg, J.J., Bouwman, A.F., 2023. Inland waters increasingly produce and emit nitrous oxide. Environ. Sci. Technol. 57, 13506–13519.
Wang, X., Peng, S., Wu, J., Zheng, K., Wang, S., Shangguan, Z., Deng, L., 2024. Simulation of the key ecosystem services changes in China's loess plateau under various shared socioeconomic pathways scenarios. Ecosyst. Heal. Sustain. 10, 1–12.
Wu, J., Liu, S., Peng, C., Luo, Y., Terrer, C., Yue, C., Peng, S., Li, J., Wang, B., Shangguan, Z., Deng, L., 2024. Future soil organic carbon stocks in China under climate change. Cell Rep. Sustain., 100179
Xing, Y., Xie, P., Yang, H., Ni, L., Wang, Y., Rong, K., 2005. Methane and carbon dioxide fluxes from a shallow hypereutrophic subtropical Lake in China. Atmos. Environ. 39, 5532–5540.
Yang, L., Lu, F., Zhou, X., Wang, X., Duan, X., Sun, B., 2014. Progress in the studies on the greenhouse gas emissions from reservoirs. Acta Ecol. Sin. 34, 204–212.
Yue, F.J., Li, S.L., Liu, C.Q., Zhao, Z.Q., Ding, H., 2017. Tracing nitrate sources with dual isotopes and long term monitoring of nitrogen species in the Yellow River. China. Sci. Rep. 7, 1–11.
Zhang, H., Chen, F., Wang, L., Wang, N., Yu, B., 2023. Reservoir inventory for China in 2016 and 2021. Sci. Data (Basel) 10, 609.
Zhang, L.W., Stanley, E.H., Ros, G.R., Dean, J.F., Wang, Q., Zhang, L., Shi, W., Xie, T., Xia, X., 2024. System-wide greenhouse gas emissions from mountain reservoirs draining permafrost catchments on the qinghai-tibet plateau. Glob. Biogeochem. Cycles 38.
Zhang, X., Zhang, Y., Shi, P., Bi, Z., Shan, Z., Ren, L., 2021. The deep challenge of nitrate pollution in river water of China. Sci. Total Environ. 770, 144674.
Zhou, F., Li, L., Zhang, K., Trajcevski, G., Yao, F., Huang, Y., Zhong, T., Wang, J., Liu, Q., 2020. Forecasting the evolution of hydropower generation. In: Proceedings of the 26th ACM SIGKDD International Conference on Knowledge Discovery & Data Mining. ACM, USA, pp. 2861–2870.
Zhou, H., Zhang, X., Liu, J., Lu, X., Sun, H., Di, S., 2021. Study on measures of preventing and reducing silting of old hydropower stations in high sediment content reservoir area. IOP Conf. Ser. Earth Environ. Sci. 768, 012004.
Zhao, X., Xu, H., Kang, L., Zhu, G., Paerl, H.W., Li, H., Liu, M., Zhu, M., Zou, W., Qin, B., Zhang, Y., 2024. Nitrate sources and transformations in a river-reservoir system : Response to extreme flooding and various land use. J. Hydrol. 638, 131491.
Zhao, Y., Zheng, B., Jia, H., Chen, Z., 2019. Determination sources of nitrates into the Three Gorges Reservoir using nitrogen and oxygen isotopes. Sci. Total Environ. 687, 128–136.
Zhou, P., Huang, J., Pontius, R.G., Hong, H., 2016. New insight into the correlations between land use and water quality in a coastal watershed of China: does point source pollution weaken it? Sci. Total Environ. 543, 591–600.